

Supporting information

Experimental

Synthesis of 1

Complex **1** has been synthesized according to a published procedure.¹ Reagents were obtained from commercial sources and used as received. Solvents were purified using standard techniques. Spectroscopic analysis and electrochemical studies have also been reported in the same paper. CuCl₂·2H₂O (3.00 mmol, 511 mg), 4-Cl-pzH (3.07 mmol, 315 mg), NaOH (6.60 mmol, 264 mg) and PPnCl (3.09 mmol, 1.775 g) were mixed in 15 mL CH₂Cl₂ at room temperature overnight. NaCl and other solids were filtered off and the filtrate was concentrated under vacuum to 5 mL. 25 mL of diethyl ether was added to crush off the solids and the cloudy ether suspension on top was discarded. This step was repeated 3 times until the ether comes off clean. The solid was then dissolved in CH₂Cl₂ and set up for crystallization by ether vapor diffusion. Dark blue-green crystals were obtained in 3 days.

X-ray Crystallography

A single crystal of **1** was mounted atop a MiteGen® Cryoloop and data was collected using a Bruker D8 Quest CMOS diffractometer at 105 K. A graphite monochromated Mo sealed tube was used as a Mo K α ($\lambda = 0.71073$ Å) source. Structure refinement was done using SHELXL on Olex2² user interface. The structure was refined as a mixture of anions containing 78% of [Cu₃(μ_3 -O)] and 22% of [Cu₃(μ_3 -OH)(μ_3 -Cl)] cores, using PART routine of SHELXL. Relevant details are shown in Table S1.

Table S1. Crystal structure determination and refinement parameters.

Empirical formula	C ₁₁₇ H _{96.28} Cl _{7.28} Cu ₃ N ₉ O _{1.72} P ₆
Formula weight	2290.43
Temperature / K	104.86
Crystal system	Trigonal
Space group	R3
<i>a</i> / Å	22.6596(11)
<i>b</i> / Å	22.6596(11)
<i>c</i> / Å	17.6051(9)
α / °	90
β / °	90
γ / °	120

Volume / Å ³	7828.4(9)
Z	3
$\rho_{\text{calc}} / \text{g cm}^{-3}$	1.458
μ / mm^{-1}	0.942
F(000)	3528.0
Crystal size / mm ³	0.352 × 0.247 × 0.15
Radiation	MoK α ($\lambda = 0.71073$)
2 θ range for data collection/°	5.96 to 52.668
Index ranges	-28 ≤ h ≤ 28, -28 ≤ k ≤ 28, -21 ≤ l ≤ 21
Reflections collected	32819
Independent reflections	7052 [$R_{\text{int}} = 0.0263$, $R_{\text{sigma}} = 0.0314$]
Data/restraints/parameters	7052/2/441
Goodness-of-fit on F ²	1.049
Final R indexes [$I \geq 2\sigma(I)$]	$R_1 = 0.0242$, $wR_2 = 0.0594$
Final R indexes [all data]	$R_1 = 0.0261$, $wR_2 = 0.0601$
Largest diff. peak/hole / e Å ⁻³	0.64/-0.47
Flack parameter	0.013(3)

Magnetic and EPR experiments

Magnetic susceptibility measurements were performed using an MPMS-5500 Quantum Design. Experimental data were corrected for the sample holder and for the diamagnetic contribution of the sample using Pascal's constants. Fits were carried out using the PHI package.³

CW EPR spectra were collected on an EMXplus spectrometer fitted with an EMX microX bridge and a Bruker ER4122SHQE cavity operating in the TE₀₁₁ mode. For low-temperature experiments the cavity was fitted with an ESR900 dynamic continuous flow cryostat and the temperature was regulated with an Oxford ITC4 servocontrol. Q-band spectra were recorded on an EMXplus spectrometer fitted with an EMX premiumQ microwave bridge and an ER5106QTW microwave resonator operating in the TE₀₁₂ mode and controlled by the Bruker Xenon software. For low-temperature experiments the resonator was fitted in an Oxford CF935 dynamic continuous flow cryostat and the temperature was regulated with an Oxford ITC503 servocontrol. The magnetic field was applied by a Bruker BE25 electromagnet using a Bruker ER082(155/45)Z power supply. For single-crystal experiments a crystal was indexed on an X-ray diffractometer and mounted on a teflon cube placed inside the EPR tube.

Fits to the EPR data and simulations were carried out with *Easyspin* v. 6.0 using custom-made routines.⁴ In particular, single-crystal spectra at each rotation were calculated for a specific set of spin Hamiltonian parameters by an auxiliary function using *Easyspin*'s *pepper* function. For the calculations we considered natural ^{63/65}Cu abundances and the same strain on the g_x and g_y tensor elements. Least-

squares fitting was carried out by a Matlab script calling the auxiliary function through Easyspin's *esfit* function. The root-mean-square deviation was calculated for the dataset consisting of all single-crystal spectra, taking care to normalize their intensities prior to the error calculations to assure equal statistical weighting. For the video showing the evolution of the transitions at different δ/Δ ratios, Zeeman plots and transitions at these conditions and at $H||z$ were plotted using Easyspin's *levelsplot* function.

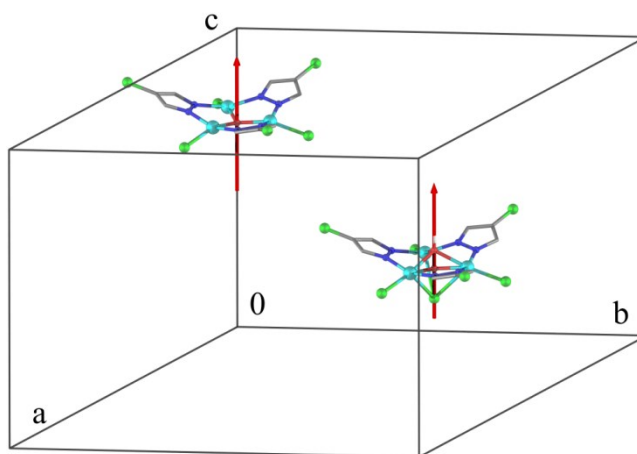


Figure S1. Partially filled unit cell of $(\text{PPN})_3[\mathbf{1a}]_{0.78}[\mathbf{1b}]_{0.22}\cdot\text{H}_2\text{O}\cdot\text{Cl}$, showing the relative orientations of two adjacent molecules, taken by convention at positions (x, y, z) for $\mathbf{1a}$ and $(1/3 + x, 2/3 + y, z - 1/3)$ for $\mathbf{1b}$. The red arrows indicate the crystallographically-imposed C_3 local symmetry axes, both parallel to the c crystallographic axis.

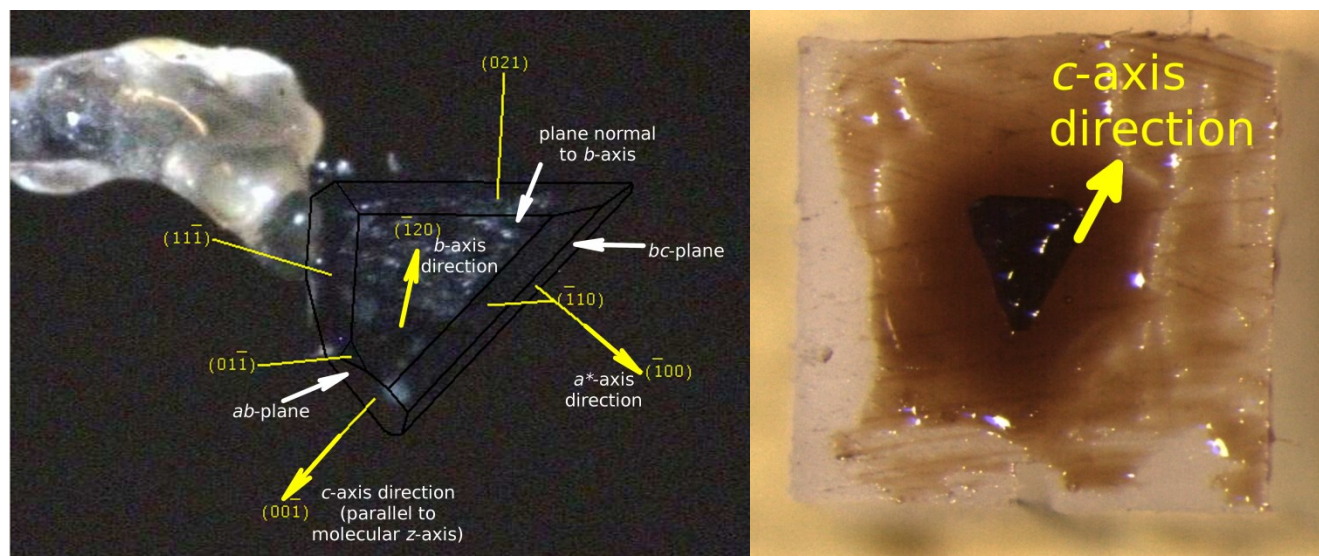


Figure S2. **Left:** Indexing of the single crystal of $(\text{PPN})_3[\mathbf{1a}]_{0.77}[\mathbf{1b}]_{0.23}\cdot\text{H}_2\text{O}\cdot\text{Cl}$ used for EPR experiments. **Right:** The single crystal placed on a teflon cube for rotation experiments.

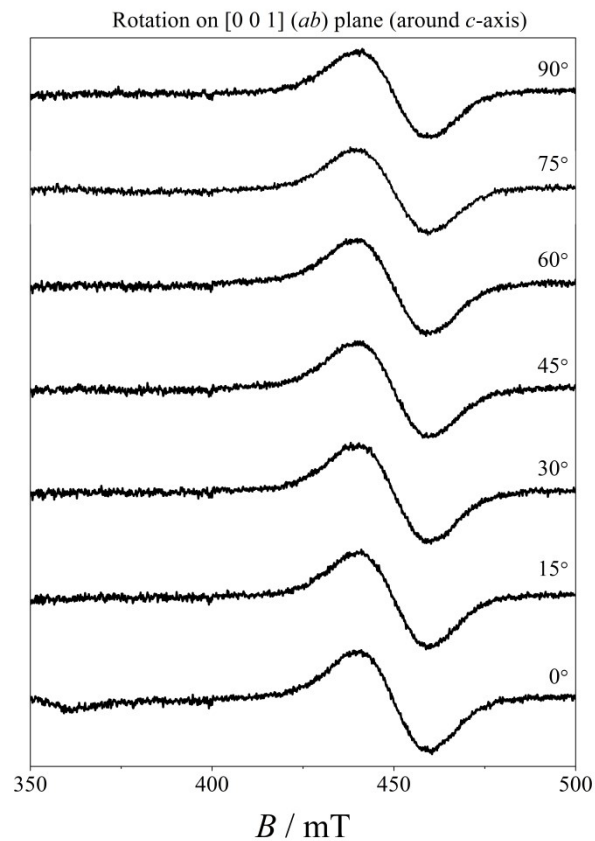


Figure S3. Rotations of the single-crystal around the c crystallographic axis ($z \perp \mathbf{B}_0$). Exp. Conditions: $f_{\text{MW}} = 9.420$ GHz, $P_{\text{MW}} = 2.03$ mW, $B_{\text{mod}} = 5$ G_{pp}.

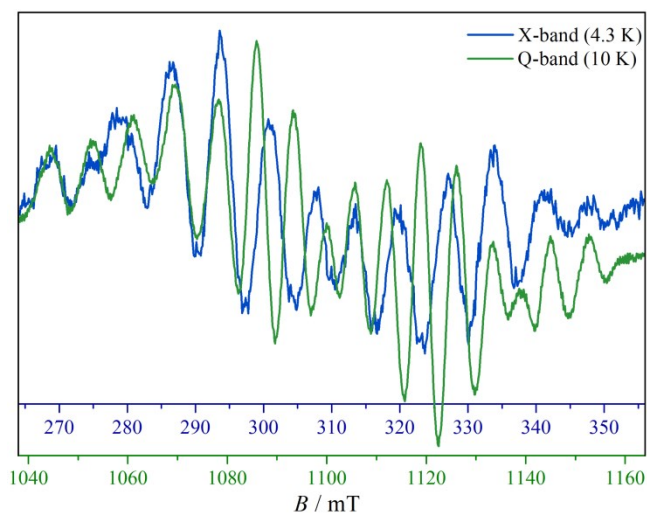


Figure S4. Comparison of the $\mathbf{B}_0 \parallel z$ single-crystal spectra at the X- and Q-bands. Experimental conditions those of Figure 4.

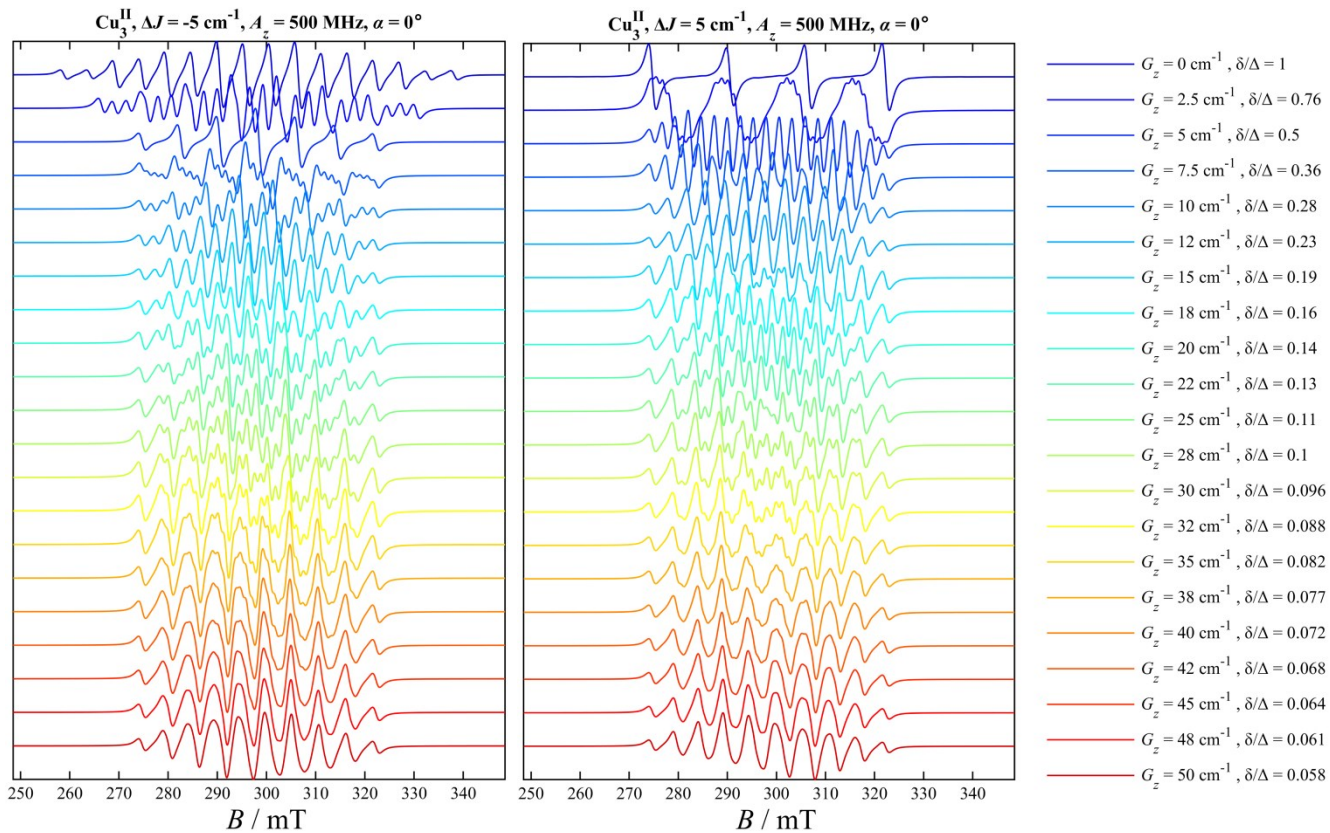


Figure S5. Simulations of the evolution of the multiline hyperfine pattern with increasing DMI (from top to bottom) based on exact full-matrix calculations of the spectra for $J = -50 \text{ cm}^{-1}$. **Left (right):** case **I (II)** corresponds to $\Delta J < 0$ ($\Delta J > 0$) leading to a 16-line (4-line) pattern in the isotropic case.

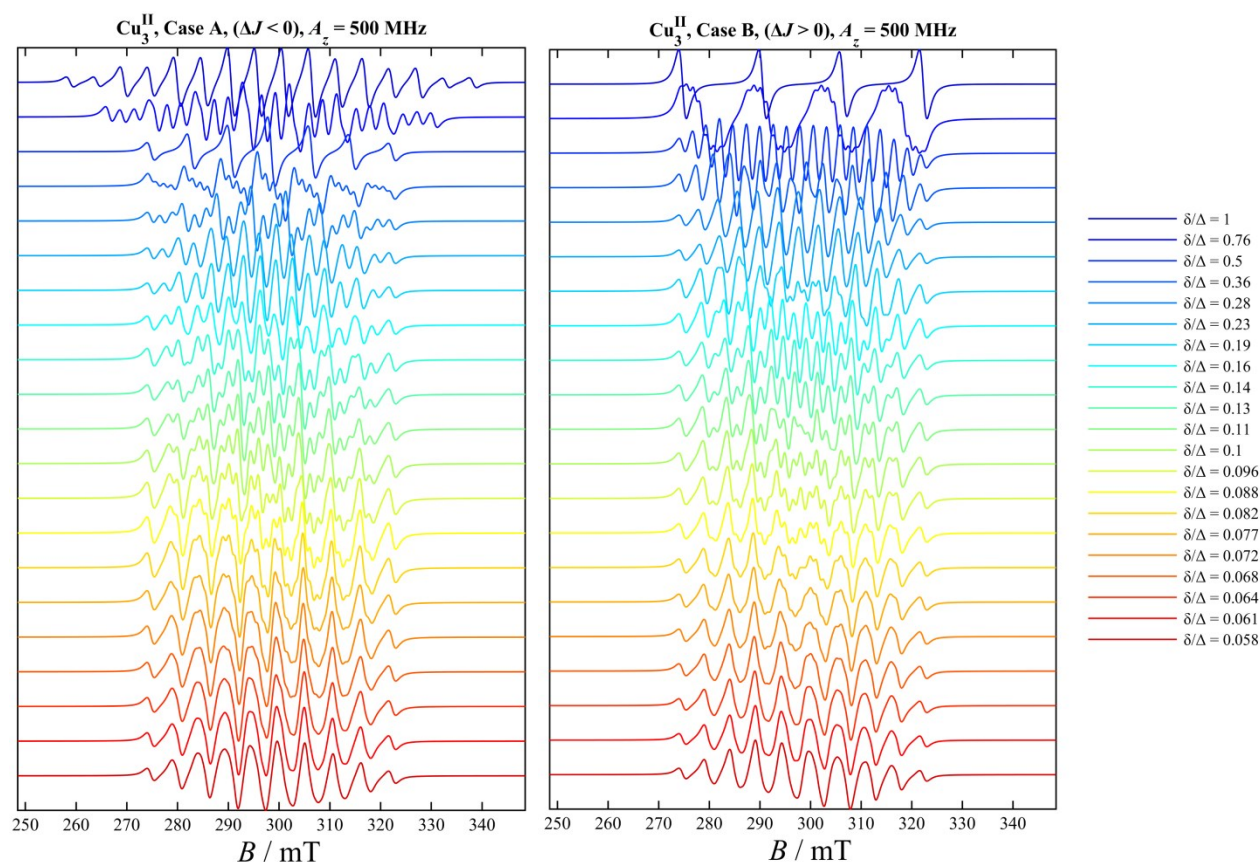


Figure S6. Simulations of the evolution of the multiline hyperfine pattern with increasing DMI (from top to bottom) based on the analytical expressions for an effective $S = 1/2$ system. **Left (right):** case **I (II)** corresponds to $\Delta J < 0$ ($\Delta J > 0$) leading to a 16-line (4-line) pattern in the isotropic case.

References

- (1) Rivera-Carrillo, M.; Chakraborty, I.; Mezei, G.; Webster, R. D.; Raptis, R. G. Tuning of the $[\text{Cu}_3(\mu\text{-O})]^{4+/5+}$ Redox Couple: Spectroscopic Evidence of Charge Delocalization in the Mixed-Valent $[\text{Cu}_3(\mu\text{-O})]^{5+}$ Species. *Inorg. Chem.* **2008**, *47* (17), 7644–7650. <https://doi.org/10.1021/ic800531y>.
- (2) Dolomanov, O. V.; Bourhis, L. J.; Gildea, R. J.; Howard, J. A. K.; Puschmann, H. OLEX2: A Complete Structure Solution, Refinement and Analysis Program. *J. Appl. Crystallogr.* **2009**, *42* (2), 339–341. <https://doi.org/10.1107/S0021889808042726>.
- (3) Chilton, N. F.; Anderson, R. P.; Turner, L. D.; Soncini, A.; Murray, K. S. PHI: A Powerful New Program for the Analysis of Anisotropic Monomeric and Exchange-Coupled Polynuclear *d*- and *f*-Block Complexes. *J. Comput. Chem.* **2013**, *34* (13), 1164–1175. <https://doi.org/10.1002/jcc.23234>.
- (4) Stoll, S.; Schweiger, A. EasySpin, a Comprehensive Software Package for Spectral Simulation and Analysis in EPR. *J. Magn. Reson.* **2006**, *178* (1), 42–55. <https://doi.org/10.1016/j.jmr.2005.08.013>.